



OTC 18219

Monitoring Primary-Depletion Reservoirs With Seismic Amplitudes and Time Shifts

A. Tura, T. Barker, P. Cattermole, C. Collins, J. Davis, P. Hatchell, K. Koster, P. Schutjens, and P. Wills, Shell Intl. E&P

Copyright 2006, Offshore Technology Conference

This paper was prepared for presentation at the 2006 Offshore Technology Conference held in Houston, Texas, U.S.A., 1–4 May 2006.

This paper was selected for presentation by an OTC Program Committee following review of information contained in an abstract submitted by the author(s). Contents of the paper, as presented, have not been reviewed by the Offshore Technology Conference and are subject to correction by the author(s). The material, as presented, does not necessarily reflect any position of the Offshore Technology Conference, its officers, or members. Papers presented at OTC are subject to publication review by Sponsor Society Committees of the Offshore Technology Conference. Electronic reproduction, distribution, or storage of any part of this paper for commercial purposes without the written consent of the Offshore Technology Conference is prohibited. Permission to reproduce in print is restricted to an abstract of not more than 300 words; illustrations may not be copied. The abstract must contain conspicuous acknowledgment of where and by whom the paper was presented. Write Librarian, OTC, P.O. Box 833836, Richardson, TX 75083-3836, U.S.A., fax 01-972-952-9435.

Abstract

In the high-porosity, poorly-consolidated turbidites of the Deepwater Gulf of Mexico (GoM), production induced compaction is the main production-drive mechanism when aquifer support is weak and prior to pressure support by secondary recovery water injection. Time-lapse (4D) seismic monitoring of this class of reservoirs has provided several new learnings. The time-lapse amplitude response of these fields can be complicated due to saturation changes (water replacing oil) inside the reservoir, rock compaction causing density and velocity changes inside the reservoir, stress relief and associated deformation of the rock outside the reservoir, and changes in reservoir fluid pressures due to pore pressure decrease. Methods that rely on time-lapse amplitude changes with offset to discriminate pressure and saturation changes can help separate and thus simplify the interpretation of some of these effects (Tura & Lumley, 1999; Landro, 2001).

In addition to 4D amplitudes, 4D time-shifts are also observed due to alteration of the stress state inside and outside the reservoir resulting from changes in the pore pressure from production. This causes a physical displacement and also a velocity change in the rocks (due to compaction in the reservoir and expansion outside). 4D time-shifts occur in areas of depletion and the overburden, and have the potential to act as indicators of compartmentalization in the reservoir. Compartmentalization information can help better place new production and injection wells, and new sidetracks for optimized field development. Travel time changes are mostly sensitive to reservoir compaction caused by depletion rather than fluid saturation changes, and as a result are simpler to interpret compared to amplitude changes. 4D time-shifts are modeled here by computing the stress field and displacements using geomechanics, and then matched to field data (Guilbot & Smith, 2002; and Hatchell et al., 2003).

In primary-depletion reservoirs, the above mentioned 4D amplitude and travel time changes are not large. Small to moderate amplitude changes manifest at the oil-water contact or in large pressure depletion areas. The travel time changes can be on the order of one to several time samples of the typical seismic sampling interval of 4 milliseconds (ms). In addition to this, particularly in the GoM, the overburden can be quite complex with large faulting, salt bodies, steep dips, near surface channels and bodies, diffractors, and overpressured regions. As a result, 4D monitoring of this class of reservoirs requires highly repeatable seismic data with very accurate positioning of sources and receivers between surveys.

In the GoM, it is often difficult to obtain high repeatability with 3D streamer surveys due to strong currents. A novel 2-boat 3-pass acquisition method to overcome acquisition repeatability issues is investigated by the Shell Mars/Europa 4D study team. Using seismic data with this new acquisition over the Mars and Europa fields in the GoM, we are able to obtain better repeatability. In addition, we are able to match amplitude changes computed from synthetic seismic (via history matched reservoir simulation models) and also travel-time changes computed from geomechanical models of these fields. The results so far have encouraged us to apply the novel acquisition method to another 12 fields in the GoM.

Mars and Europa Fields

Field data from Mars and Europa are used to demonstrate the concepts discussed in this paper. Mars is a large field in water depths of approximately 4000ft with approximately 500 million barrels of recoverable oil still remaining from 18 vertically stacked producing reservoirs. Most production is from 4 main reservoirs, with up to 7000psi pressure depletion, with the deepest one being the largest. Water flood was started in 2004 to recover remaining reserves. Time-lapse surveys of this field are important to monitor the water flood and detect compartmentalization.

Europa is subsea completed and connected to the Mars platform. It has two producing reservoirs, with up to 4000psi pressure depletion, and has been undergoing primary depletion since January 2000. Well performance indicated that both producing reservoirs are compartmentalized by small-scale faults and production problems have been encountered due to well failures and fluid flow impairment. Time-lapse seismic is used in this field to detect compartmentalization and movement of the oil water contact.

4D Amplitude Changes

A 3D monitor streamer survey was acquired at Europa in mid 2002 for time-lapse purposes. Although data repeatability is not optimal, there are no surface obstructions, interference from salt, or numerous stacked depleting reservoirs to complicate the 4D analysis. Time-lapse amplitude changes on stacked data, that are consistent in time-lapse offset gathers, are seen near Well 2 and are related to saturation changes, with oil being replaced by water (Figure 1). Well 2 is in fact the largest producer and water cut has reached 40%, confirming the 4D observations.

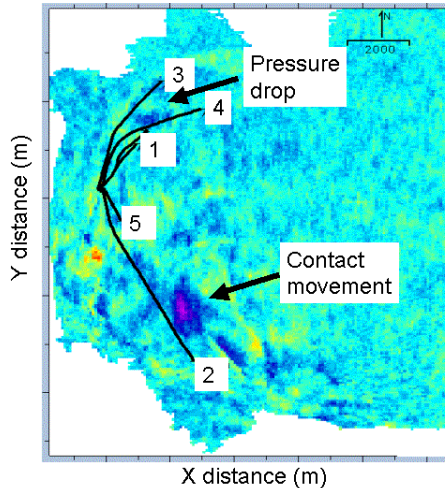


Figure 1: Time-lapse stacked amplitude (difference) attribute over Europa field, A reservoir. Blue and purple colors show hardening and yellow and red show softening. Water contact movement can be seen at Well 2 (hardening due to oil being replaced by water) that is confirmed by increased water cut at 40% at this well. Pressure drop up to 4,000psi near Well 3 and up to 1,000psi near Well 4 shows small amplitude changes (hardening) near these wells.

Time-lapse seismic amplitudes show small changes even though the reservoir has depleted by several thousands of psi (Figure 1). When compared to velocity vs. effective stress measurements on cores from the Europa field, the observed amplitudes changes are less than expected. This can be due to acquisition non-repeatability, complexity of the time-lapse amplitude response, and/or core data reliability (Nes et al, 2002). In addition, the laboratory core data measurements are under uniaxial-strain conditions, while the Europa sands may undergo a different stress path. The amplitude response can be complicated because there are several mechanisms operative in parallel, all affecting the seismic signal: Water replacing oil, rock compaction causing density and velocity changes inside the reservoir in the sands and outside the reservoir in the shales (due to stress relief and associated deformation), and also changes in reservoir fluid pressures due to production.

4D Travel time Changes

4D travel time changes result from alteration of the stress field inside and outside of the reservoir due to production induced pressure decrease in the reservoir, causing a physical displacement and also a velocity change in rocks (due to compaction/expansion) which translates to a time-lapse time-shift (Landro & Stammeijer, 2002). For a depth of z_{ref} from

the earth's solid surface (depth of 0), the time-shifts for a vertical ray in a one-dimensional medium can be given as:

$$\Delta t = 2 \int_0^{z_{ref}} E_{zz}(z) / V_0(z) dz - 2 \int_0^{z_{ref}} \Delta V(z) / (V_0(z))^2 dz .$$

The two terms show the time-shifts due to strain (E_{zz}) and velocity (ΔV) variation in the subsurface, where V_0 is the original (pre-depletion/deformation) velocity and z is depth. For marine seismic data, time-shifts due to changes in the water thickness, from subsidence at the water bottom, also needs to be added to time-shifts calculated from the above relationship. The first term in the integral shows the change in length of the length element, $E_{zz} dz$, due to reservoir-compaction-induced stress changes in the overburden. The strain term is a geometrical term describing the movement of the layer boundaries (with respect to an external reference system), with compaction in sands and vertical expansion in the shales above, between and below compacting reservoirs. The second term gives the local propagation time change due to the variation in the local velocity from strain/stress changes. It can be viewed as due to an "effective" length change, $(\Delta V / V_0) dz$. This second term can be computed in one of two ways given that stress and strain changes have been computed through geomechanical simulation. One is through using a velocity-stress relationship for the sands and a separate velocity-stress relationship for the shales to compute velocity changes, given that stress changes are known from geomechanical simulation. In these computations, assuming vertical rays, the stress term is the change in vertical effective stress. Figure 2 provides a mental model of how changes in vertical effective stress, due to pore pressure change from depletion in the reservoir, translate to velocity changes and thereby time-shifts. A second method is to replace the velocity term $(\Delta V / V_0)$ in the above equation by a strain term ($R E_{zz}$). This is discussed in detail in the article by Hatchell and Bourne, 2005, and Schutjens et al., 2005. In this case, once R is determined for the sands and shales, only the strain field is used from geomechanical simulation to compute time-shifts.

To model time-shifts for a particular field, a 3D geomechanical model is built to compute the stress and strain changes, given the depletion from reservoir simulation between baseline and monitor data acquisition times. Geomechanical models were built for both the Mars and Europa fields. Initially 3D layer boundaries based on geology outside of the reservoir areas are introduced into the model. Then the reservoir geometric definition and pressure variations over time are imported from the reservoir simulator. In this approach the geomechanical simulator is not coupled to the reservoir simulator (first the reservoir simulator is run and then the geomechanical simulator uses this as input for its run). Initial conditions of pre-production total vertical stress were estimated and set from well log density data. Initial total horizontal stress conditions, in both lateral directions, are set using a constant ratio between total vertical stress and total horizontal stress and relaxing this model to equilibrium using zero lateral strain boundary conditions.

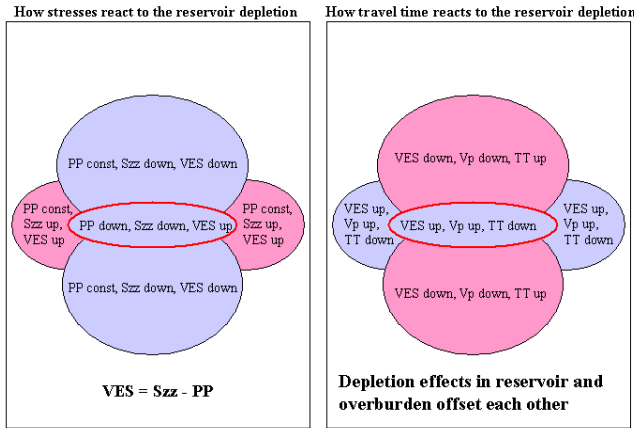


Figure 2: Mental model of how change in pore pressure due to production can cause changes in velocities (and bulk density), and thereby create time-shifts in 4D seismic. Reservoir is red ellipse in the center. Pore pressure reduction at the reservoir (PP) increases vertical effective stress (VES). Outside the reservoir VES decreases. Stress arching at the boundaries of the reservoir increases vertical stress (Szz) and thereby VES. P-wave velocity (Vp) (S-wave velocity and bulk density) change and thereby travel time (TT) changes can be calculated from VES changes, provided the rock physics relationships are known that relate the change in effective stress in reservoir and over/under/sideburden to the local velocity changes.

The geomechanical model is populated with static mechanical properties of Young’s modulus and Poisson’s ratio. These are calculated in the sands based on field measurements of time-lapse casing strain, laboratory compaction measurements of core samples, thin sections, well log data, and measurements of shear fracture strength. Such measurements on shales are scarce and empirical relationships and dynamic measurements are used to calculate static Young’s modulus and Poisson’s ratio.

The geomechanical simulator uses finite-element computations to compute the stress and strain changes in the model due to depletion at the reservoirs. Figure 3 shows a cross section of the vertical displacement for the Europa field, with two producing reservoirs, computed between the baseline and monitor seismic acquisition times. As the sands compact due to production, the shales are expanding. Figure 4 shows the change in total vertical stress (TVS) from geomechanical computations. TVS decreases above the reservoir and increases at the edges of the reservoir due to stress arching. As discussed previously, a decrease in the TVS (overburden and underburden) indicates a velocity slowdown and an increase in TVS (inside the reservoir and at reservoir boundaries) indicates a velocity speedup.

The velocity-stress relationships for the sands are obtained from laboratory core measurements where samples are deformed under uniaxial-strain conditions, with only vertical compaction and no horizontal deformation. While analytical and numerical modeling indicates that this strain mode is a good approximation of the deformation in deep laterally extensive reservoirs, the actual stresses and strains due to

depletion may be different, in particular at the edges of the reservoir and any intra-reservoir compartments.

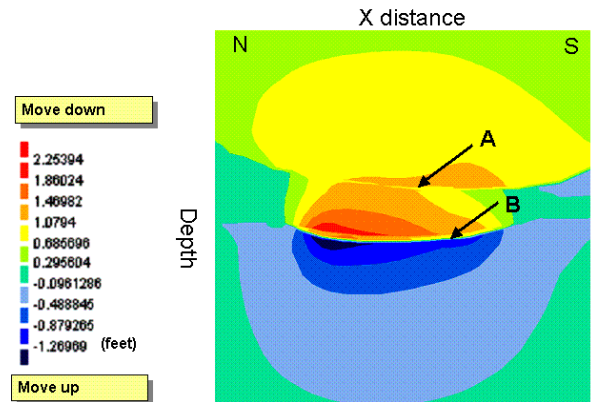


Figure 3: Vertical displacement from depletion of two Europa reservoirs (A and B) between baseline and monitor in North-South cross-section view. Note that the shales just above reservoir B move down by about 2 feet, whereas the seafloor moves down by only about 0.5 feet. This indicates that the overburden stretched vertically by about 1.5 feet.

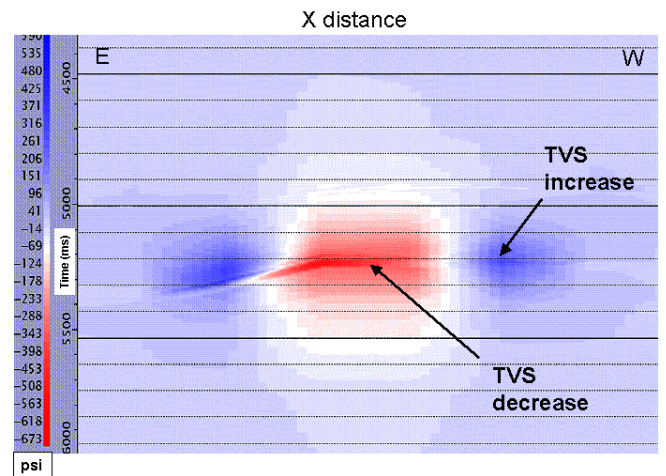


Figure 4: Total vertical stress (TVS) change in East-West cross-section between baseline and monitor at Europa due to depletion at reservoir (in middle). Red areas show TVS decrease around the reservoirs and blue areas show TVS increase at boundaries of the reservoirs due to stress arching.

Velocity-stress measurements on shales are very scarce. There is little shale core in Mars and Europa, and laboratory deformation experiments on the low-porosity/low-permeability shales are difficult to perform. Also, pore-pressure-diffusion effects inside the samples lead to gradients in effective stress that change as a function of time, and long hold times are needed (at constant total stress) to stress-equilibrate the samples. More in-situ and laboratory measurements on sands and shales can help better constrain computed time-shifts. Substituting strain for the velocity term in the time-shift equation above and calibrating the R value (see previous section) based on field observations is a way to bypass the requirement for a velocity-stress relationship.

The time-shift equation is discretized based on layer boundaries in the geomechanical model and contributions from strain and velocity terms are summed up to compute time-shifts at each depth in the model. Figure 5 shows the time-shifts (between baseline and monitor) computed along a vertical path using the geomechanical simulation results for the Mars field. Note the slowdown in the overburden and speed up in the reservoir. In the computations the full stress tensor is calculated. It is found sufficient to compute time-shifts along a vertical ray using only the total vertical stress component of this tensor.

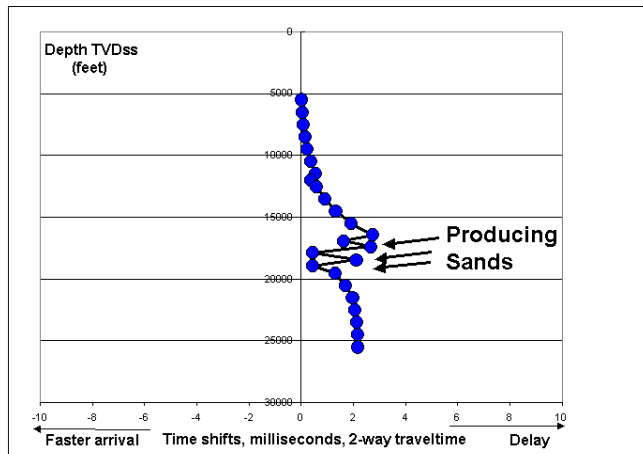


Figure 5: Time-shifts computed along a vertical path with displacements and stresses obtained from geomechanical simulation for the Mars field. Note velocity decrease in shales (slowdown) and velocity increase in sands (speed up).

Novel 2-boat 3-pass time-lapse acquisition

Highly repeatable time-lapse seismic data are required to obtain time-shifts from field data, given that we are looking for time-shifts on the order of a few milliseconds. This is also true for amplitude analysis when the time-lapse signal is small (i.e. primary depletion). 4D streamer surveys shot in the GoM have evolved over time. In the early years of 4D, two legacy surveys, shot even in different directions, were used to show the feasibility of 4D with marginal results. Later on surveys were shot that repeated the acquisition direction but did not reproduce shot or receiver locations. Although the results improved, quantitative analysis of such data was still not possible. In a period between 2000 and 2001, Shell shot several 4D surveys in the GoM that repeated acquisition direction and to a certain extent shot and receiver locations. From these surveys we observed the following:

- Due to unpredictable and highly variable eddy currents in the GoM, the mid and far offsets are difficult to repeat, with up to 15 degrees of feathering between baseline and monitor cables. An example of this is shown in Figure 6 where we can see up to 1000m differences between baseline and monitor receiver locations at far offsets.
- The overburden in the GoM can be complex and as a result minor shot and receiver non-repeatability can result in significantly different ray paths. Figure 7 shows the complexity of the overburden over the Europa field with faults, channels, and scatterers.

- Undershoots in areas near platforms increase the operational complexity of acquiring meaningful 4D streamer data.

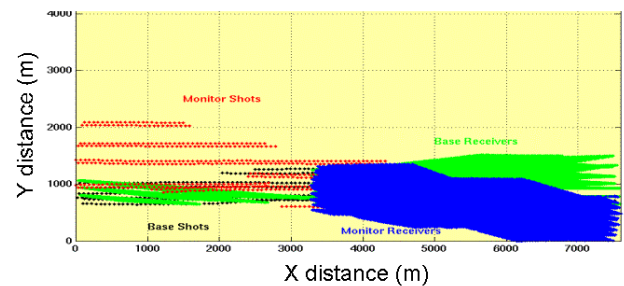


Figure 6: Feathering in the Gulf of Mexico due to eddy currents causes large repeatability errors as offsets increase. Blue continues lines are the monitor receiver cables and green continuous lines are the baseline receiver cables. 1000m differences between baseline and monitor receiver locations can be seen at far offsets.

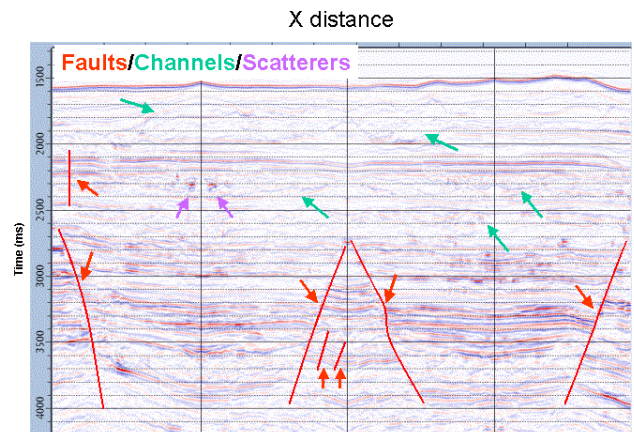


Figure 7: Overburden complexity over the Europa field showing faults, channels, and scatterers. Note that the reservoir is at 5 seconds (1 second further down).

The operational challenge is to obtain highly repeated seismic data in a challenging environment in order to detect small magnitude signals with confidence that can be used reliably in well planning and production optimization.

In early 2005, six seismic lines from baseline surveys for the Mars (4 lines) and Europa fields (2 lines) were repeated. The lines were chosen so as to have minimal dip and in areas of significant production. To repeat the 6km baseline cable length, 2D lines were acquired with a two-boat operation: a separate source and receiver cable boat. Shot locations were repeated three times with short 2km receiver cables in order to record near, mid, and far offset ranges accurately. The receiver

at the mid-point of the 2km cable was positioned to repeat a receiver location at the corresponding offset of a baseline cable. Figure 8 shows how the receiver cable was repeated with three passes. In the middle of the 2km monitor cable positioning errors are less than 3m's whereas near the ends of the cable they can range from 10m's to 80m's depending on currents. This is a significant improvement in repeatability compared to conventional 6km streamer acquisition where the receiver locations can vary up to 1km at far offsets (see Figure 6). For processing of the data, each trace from the 3-pass monitor data is paired with a trace from the multi-cable baseline data according to geometric proximity, and the paired data set is processed with identical parameters.

subtracted out other than changes in the producing reservoir. Time-lapse amplitude synthetics generated using the reservoir model and dynamic data for this shallow Mars reservoir with large production shows a good match to the field data. A further quality check of the repeatability is to look at prestack amplitudes. Figure 11 shows pre-stack RMS amplitudes from a gated window centered at 4 seconds, just above a reservoir. From this figure we see that the overburden transmission imprint (see Hatchell, 2000) is well repeated as seen by the identical imprint on both baseline and monitor data. The actual amplitude values on top of this overburden imprint have decreased due to production at this level and reduction in impedance contrast with the shales between baseline and monitor (causing dimming).

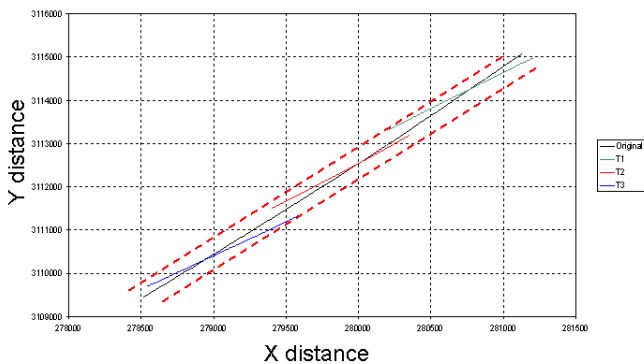


Figure 8: 2-boat 3-pass time-lapse acquisition. The 6km baseline cable is shown in black. During each pass of the monitor survey, the first boat repeats the shot location. The second boat tows the 2km cable making sure that the center of the cable intersects with the center of the 2km portion of the baseline cable. The acquisition is repeated 3 times for the near (blue), mid (red) and far (green) offset ranges of the baseline cable.

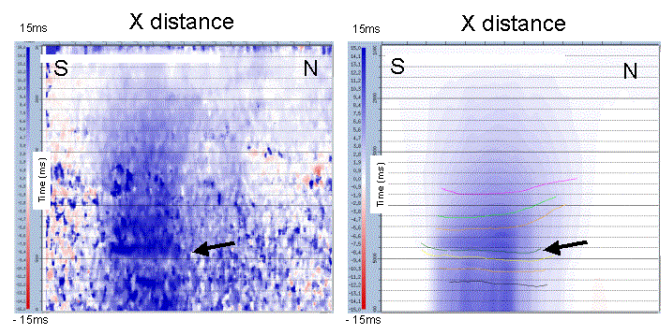


Figure 9: Comparison of time-shifts at Mars observed from stacked field data (left) and calculated from geomechanical model (right) using 2-boat 3-pass monitor acquisition. Both field data and geomechanical computations show up to 15ms time shifts with similar shape. Colored horizons on right show the producing intervals.

Time-shifts and amplitudes from 2-boat 3-pass acquisition

The measured time-shifts from the Mars field along one of these 2D repeat lines is compared to the time-shifts calculated from the geomechanical simulation in Figure 9. Time shifts are computed from windowed cross-correlations of baseline and monitor data. Details of the construction of the Mars geomechanical model are give in Schutjens et al., 2005. From this comparison we see that the time-shifts observed from field data are of the same order as the time-shifts computed using the geomechanical model. The time-shifts are large (15ms) due to the large amount of depletion (up to 7000psi) over stacked reservoirs with net thicknesses up to 200ft. Further to this, the shape of the time-shifts is also consistent between the model and field data. The large production indicated by an arrow in this figure can also be clearly seen from field data time-shifts. Note the increase in time-shifts with depth (slowdown from baseline to monitor) consistent with Figure 5. The remaining three repeat lines also show a good match to the time-shifts computed from the Mars geomechanical model. Time-lapse amplitude differences, after removal of time-shifts, are shown in Figure 10. The difference data (on the right) shows that most events in the baseline data (on the left) have

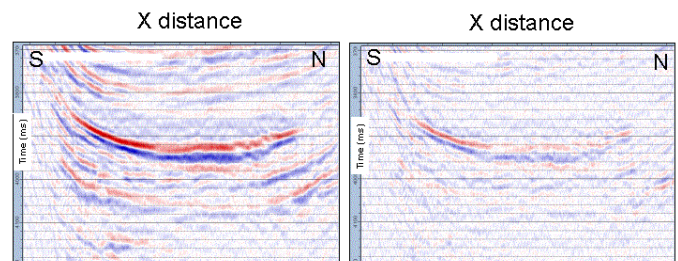


Figure 10: Mars baseline amplitude (left) and time-lapse difference amplitude (right) of stacked data from 2-boat 3-pass monitor acquisition. Time-lapse changes on the right are at a shallow producing reservoir.

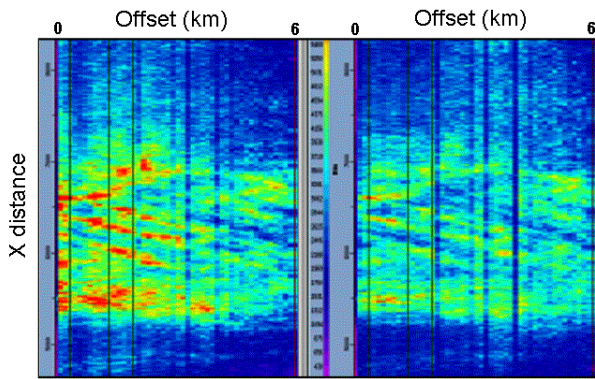


Figure 11: Mars baseline (left) and 2-boat/3-pass monitor (right) pre stack RMS amplitudes from a gated window centered at 4 seconds along the inline (Bin) direction. Note repeatability of diagonal overburden transmission imprints on both baseline and monitor data. The actual amplitude values on top of this imprint have decreased due to production at this level.

Seismic data quality at Europa (baseline and monitor) starts to deteriorate significantly after 4 seconds due to overburden complexity. The reservoir is located at 5 seconds and amplitudes are noisy at this time interval. Time-shifts observed from one of the 2-boat/3-pass monitor lines at Europa are shown in Figure 12. Time-shifts from the field data (left) and geomechanical simulation (right) both show changes up to 8ms. This is significantly less than the time-shifts observed at Mars since at Europa we have only two stacked reservoirs that are producing with up to 4000psi depletion. In addition to the magnitude, the shape of the slowdown matches the field data observation. The field data shows local areas of red spots (speeds ups). These are at locations where the seismic data shows steep dips and diffractions, and are artifacts caused by data quality and seismic imaging issues.

Time-lapse amplitude changes, after removal of time-shifts, along the second Europa 2D line are shown in Figure 13. As mentioned earlier, the Europa data is noisier than the Mars data (compare to Figure 10). When compared to the baseline data (left), the difference data shows that amplitudes outside the producing reservoir are subtracted out indicating the high quality of the time-lapse differences. Time-lapse changes along this 2D line are only at the deeper reservoir B (second orange line) consistent with production at this location. Hardening (blue) can be seen to the left of the Oil Water Contact (OWC) on the difference section. Softening (red) in the aquifer is due to free gas in the water from pressure decline.

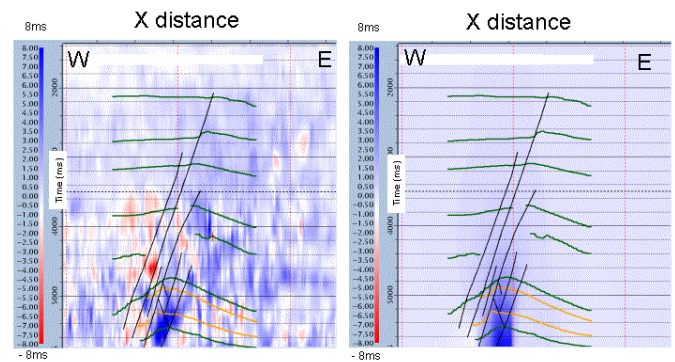


Figure 12: Comparison of time-shifts at Europa observed from stacked field data (left) and calculated from geomechanical model (right) using 2-boat 3-pass monitor data. Both field data and calculated time-shifts show up to 8ms changes with similar shape. Time-shifts at Europa are smaller than at Mars and the 2D data is noisier. Areas of large red changes in field data are caused by data quality and seismic imaging issues related to steep dips and diffractions. Orange colored horizons on right show the two producing intervals.

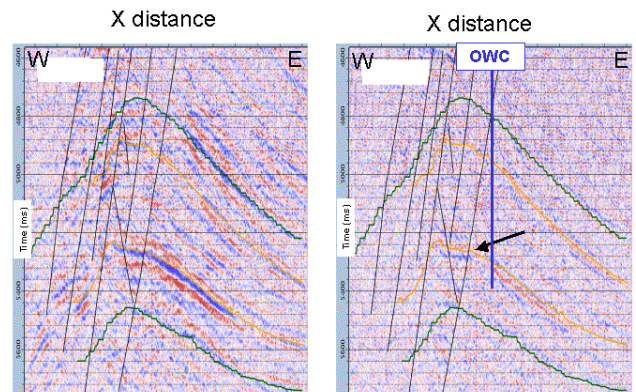


Figure 13: Europa baseline amplitude (left) and time-lapse difference amplitude (right) of stacked data from 2-boat 3-pass monitor acquisition. Changes on the right are only at the deeper producing reservoir (second orange line). Hardening (blue) in the reservoir (left of OWC) due to compaction and softening (red) in water leg (right of OWC) due to free gas.

Conclusions and future plans

4D monitoring of primary depletion in the GoM requires highly repeatable seismic data with very accurate repeat positioning of sources and receivers between surveys. The main reasons for this are the small amplitude and time-shifts that need to be measured, and the structural complexity of the overburden and requirements on ray path repeatability. Eddy currents in the GoM are a key operational challenge to obtaining accurately repeated receiver locations.

With the novel 2-boat 3-pass short cable acquisition, we are able to obtain time-shifts from seismic data that are intuitive,

agree with the position of the depleting/compacting reservoirs, and show a good match with timeshifts calculated from geomechanical models incorporating our current understanding of rock physics. In addition, clear amplitude changes can be observed that matches our synthetic models. 4D monitoring at Mars and Europa has been significantly de-risked and seismic repeatability stands out as a key prerequisite for high quality 4D data. The 2-boat, multi-pass method will be extended to multi-cable 3D surveys for time-lapse purposes. This extension is expected to allow quantitative interpretation of amplitude changes and time-shifts spatially. Such information will impact field development and optimization (detecting compartments, better placing wells, etc.) in primary depletion reservoirs.

As a result of our experience at Mars and Europa, the 2-boat 3-pass acquisition has been applied to an additional 12 GoM fields along 2D repeat lines in order to calibrate time-shift and amplitude changes. In addition, a 2D ocean bottom cable (OBC) has been installed and is being tested for time-lapse repeatability in record water depths. Successful results of the OBC may lead to field wide deployment.

Time-lapse travel time changes can be incorporated into a conventional closing-the-loop workflow with the objective of updating the static and dynamic reservoir model to match production data, time-lapse amplitudes, and time-lapse time-shifts. Geomechanical simulation is now an integral part of the workflow: Updated fluid-flow simulation results are input in the geomechanical simulator to compute 3D-volumes of stress, strain and displacement changes as a function of time, and these are in turn used to compute the density and acoustic wave velocity changes that will control the depletion/compaction-induced acoustic impedance variation and timeshifts. This can be done manually in sequence: history match production at wells, use in amplitude and time-shift match, or formulated as an optimization problem for updating the reservoir model so as to fit production, time-lapse amplitude and time-shift data (Figure 14). This integrated workflow of reservoir simulation, geomechanics, and seismic modeling is seen as a key component of being able to build accurate reservoir and geomechanical models. Reliable reservoir models are used to predict future reservoir behavior. Further, reliable geomechanical models can be used to design optimal well paths (in terms of mechanical borehole stability), extend the production lifetime of the wells, and help to optimize well locations, in particular in settings with stacked depleting reservoir where deeper objectives are being explored.

Acknowledgements

The authors would like to thank Shell management for supporting this work and Shell Mars and Europa assets and our partners (BP, ENI, ConocoPhillips) for facilitating its publication. The options expressed in this article do not necessarily reflect the views of each of the aforementioned partners. We also thank Annemieke van den Beukel, Kees Hindriks, Juun van der Horst, and Denis Prokofiev for some of the discussions, model building, and computer codes used in this study.

Closing the loop Workflow

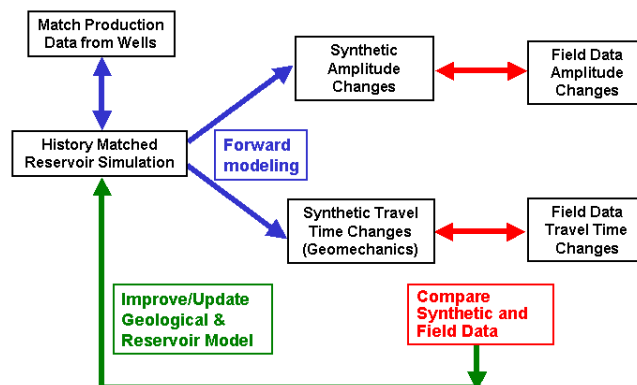


Figure 14: Closing the loop workflow with the objective of updating the static and dynamic reservoir model to match production data, time-lapse amplitudes, and time-lapse time-shifts (via geomechanical simulation). This can be done sequentially or formulated as a single optimization problem for the reservoir model to fit all three types of data. Inclusion of geomechanical modeling and matching time-shifts in this workflow reduces uncertainty and increases accuracy of predictions.

References

- Tura & Lumley, 1999, Estimating pressure and saturation changes from time-lapse AVO data, SEG Expanded Abstracts.
- Landro, 2001, Discrimination between pressure and fluid saturation changes from time-lapse seismic data, Geophysics.
- Guilbot and Smith, 2002, 4-D constrained depth conversion for reservoir compaction estimation: Application to Ekofisk field, TLE March issue.
- Hatchell et al., 2003, Whole earth 4D: monitoring geomechanics, SEG Expanded Abstract.
- Nes et al., 2002, The reliability of core data as input to seismic reservoir monitoring studies, SPE 65180.
- Schutjens et al., 2005, Reservoir monitoring with seismic time-shifts: Geomechanical modeling for its application in stacked pay, IPTC 10511.
- Landro & Stammeijer, 2002, Quantitative estimation of compaction and velocity changes using 4D impedance and travel time changes, Geophysics.
- Hatchell and Bourne, 2005, Rocks under strain: Strain-induced time-lapse time shifts are observed for depleting reservoirs, TLE December issue.
- Hatchell, 2000, Fault wispers: Transmission distortions on prestack seismic reflection data, Geophysics.